CHAPTER 3

Effect of length on the transport and magnetic properties of diradical substituted molecular wires

Abstract

In the third chapter we investigate the effect of the length of unsaturated organic molecular wires and radical substituted wires on the conduction properties of hybrid devices. At the same time, we also study the effect of length of unsaturated radical substituted organic molecular wire on the magnetic properties. It was found that the value of magnetic exchange coupling constant (*J*) depends on the distance between spin centers. In order to measure the transmission characteristics of these conjugated molecular wires, we have designed a molecular bridge structure where the phenyl based molecular system containing conjugated multiple bonds of varying length is used as a bridging fragment between two semi-infinitely widened Au_9 fcc clusters along Au(111) direction. A state of the art non-equilibrium Green's function (NEGF) method coupled with the density functional theory (DFT) based approach has been applied on this two-probe molecular bridge system to understand its electrical transport characteristics. It was observed that the molecular wires with smaller length show higher transmission. The transmission spectra of the ferromagnetically coupled diradical based molecular wires show similar behavior to those of the wires without any substitution. Hence, there is no effect of radical substitution on transport properties for ferromagnetically coupled diradical based molecular wires, whereas for antiferromagnetically coupled systems, the scenario is different.

3.1 Introduction

The term molecular wire is usually employed in molecular electronics to signify molecular scale objects which conduct electrical current with a highly preferential axis for conduction. Electrical conduction properties of molecular wires have been the focus of many studies in recent years.[1-4] Individual molecular wires are divided into two categories.[1] The first category is based on n-alkane chains [CH_3-$(CH_2)_{n-1}$] which have large (~6 eV or greater) band gap separating their highest occupied molecular orbital (HOMO) and their lowest unoccupied molecular orbital (LUMO) and are relatively insulating.[5,6] The second category is based on conjugated molecules that have a small (2-4 eV) HOMO-LUMO gap and behaves like ordinary semiconductor.[7-9] This second category of molecules are rigid and possess delocalized π-electrons. Jalili et al. investigated the effect of the length of the molecular wire on the conduction spectra of organic nanowires,[3] where the *I-V* curve for thiophenthiol based systems is non-ohmic in nature. Recently, a hybrid device is designed where gold nano particles are connected by saturated organic molecules of different lengths (alkanedithiol chains)[2] and it is observed that the conductivity increases with the length of the molecule. Electron tunneling through molecular wire has also been studied as a function of the length and chemical structure of the molecule by Magoga et al.[4] They have found that the tunneling phenomenon through a molecular wire relies on the damping factor and the contact conductance. The effect of bond length alternation on transport behavior has also been experimentally and theoretically demonstrated.[10] A study of charge and spin transport through *para*-phenylene oligomers reveals that the oligomeric *para*-phenylene bridge can act as a molecular wire for the charge recombination reaction. The rate of charge transport through such molecules decreases exponentially when the super-exchange mechanism dominates.[11] The decay constants (β) of diradical substituted conjugated molecular wires have been studied by Nishizawa et al. and they found that β is well correlated with the electronic transmission.[12]

In this work we investigate the transport property of two molecular wires of different lengths (Figure 3.1) to show the effect of the length of the wire on the electrical transport property. In this context we have designed six diradicals (Figure 3.2) by substituting methylene radical at different positions in molecular wire 1 to generate series 1 and similarly ten diradicals based on molecular wire 2 to generate the systems of series 2 (Figure 3.3) to study the effect of spin polarization on the transport property and the dependence of magnetic coupling on the distance between the radical centers. The wires we have studied here are addition polymers, and such polymers are important for application in the electronic industry.[13] The effects of entropy, the amount of molecules and their root-mean-square end-to-end distance on the physical properties of polymers are very important issues and these points were properly discussed by Lu et al.[14,15]

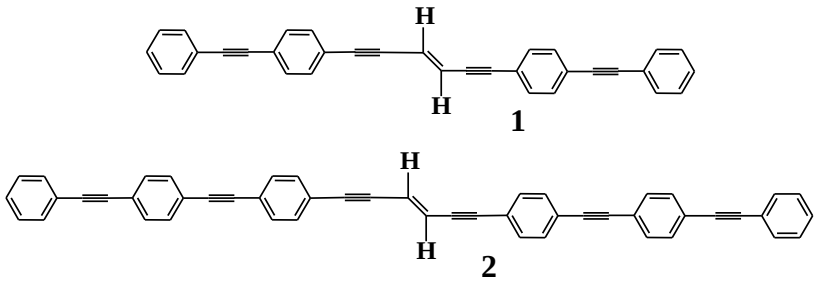

Figure 3.1 Two molecular wires (1 and 2) on which transport calculations have been carried out.

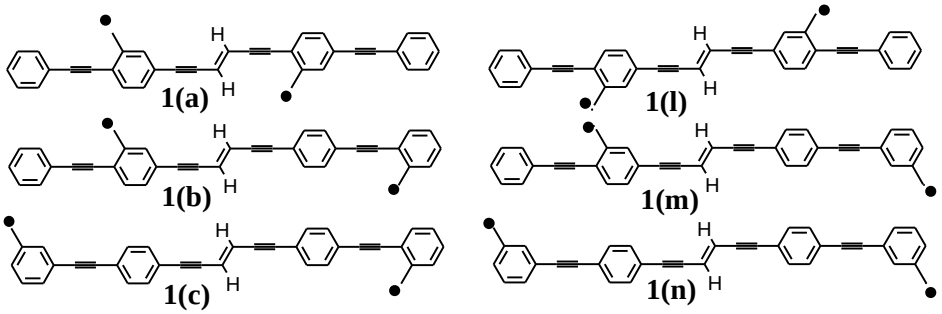

Figure 3.2 Designed diradical based molecular wire 1.

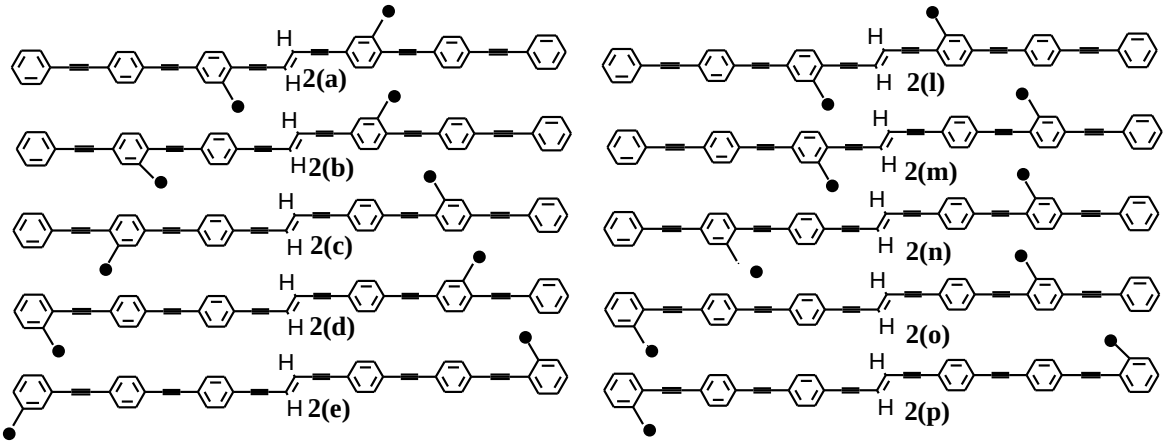

Figure 3.3 Designed diradical based molecular wire 2.

3.2 Theoretical and computational methodology

In order to determine the transport properties of the system, we need to describe the finite left electrode-molecular region-right electrode part of the infinite system. For this purpose, the gold-cluster-dithiolate-gold-cluster system has been divided into three sub systems: left gold cluster, central dithiolate, right gold cluster as

illustrated in Figure 3.4. Wires with radical substitutions are also treated in similar manner. The magnetic properties of the diradicals are calculated on the structures without –SH and gold cluster.

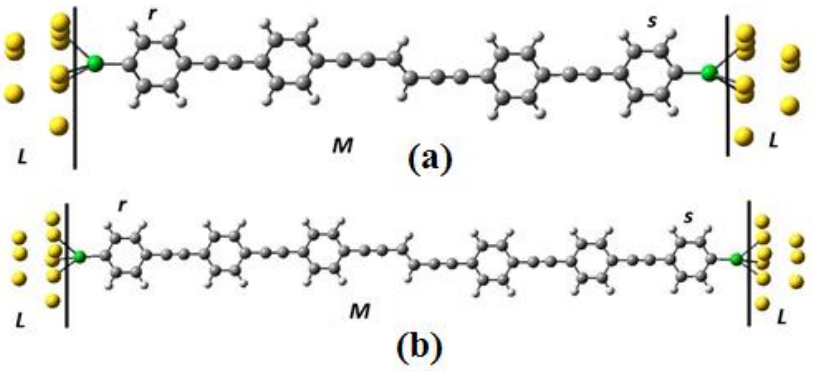

Figure 3.4 (a) and (b) are the Au-molecule-Au two probe structures designed primarily for the transport calculation. The gray, white, yellow and green colors represent carbon, hydrogen, gold and sulfur atoms respectively. *r* and *s* are two different sites of the molecular wire.

We calculated the transmission property using ARTAIOS code developed by Herrmann et al.[16,17] In this approach the dithiol molecule has been optimized in the unrestricted DFT framework with B3LYP functional and 6-31G(d,p) basis set using Gaussian09 quantum chemical package[18] and then the hydrogen atoms are stripped off and the resulting neutral dithiolate is placed between two Au_9 fcc clusters. The bond length between sulfur and Au (111) surface has been chosen to be 2.48 Å with Au-Au distances of 2.88 Å as in extended gold crystals. Fock and overlap matrices required for the transport calculation is obtained by single point calculation in Gaussian09W program package. For the transport calculation we employ B3LYP functional and the LANL2DZ basis set to avoid ghost transmission.[17] Transmission function is calculated within the Landaur approximation based on a Green's function approach using the post processing tool ARTAIOS.

Yoshizawa and coworkers have developed an orbital rule to predict the right connections between the molecule and the electrodes.[19,20] The rule is, (1) the sign of the product of the orbital coefficients at sites *r* and *s* in the HOMO should be different from the sign of the product of the orbital coefficients at sites *r* and *s* in the LUMO, (2) sites *r* and *s* should have the large amplitude of HOMO and LUMO. We computed the coefficients of HOMO and LUMO of both the wires (in Figure 3.5) that are given in Table 3.1 and a right connection has been made between the molecule and the electrodes following the Yoshizawa's rule.[19,20]

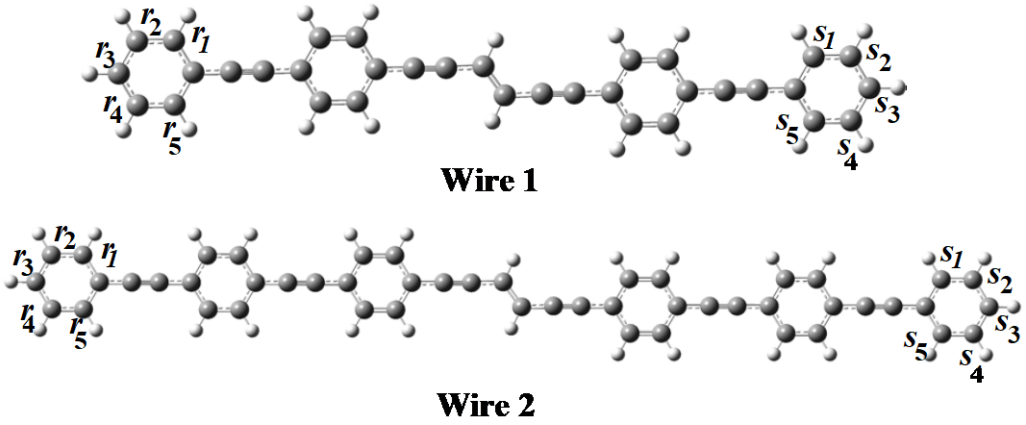

Figure 3.5 Molecular wire1 and molecular wire 2.

Table 3.1 Orbital coefficients for molecular wire 1 and wire 2 (B3LYP/6-31G(d,p)).

Site	Orbital	Molecular wire 1		Molecular wire 2	
		HOMO	LUMO	HOMO	LUMO
r_1	$2p_Z$	0.0725	0.0708	-0.0477	-0.0408
r_2	$2p_Z$	-0.0205	0.0142	0.0129	-0.0071
r_3	$2p_Z$	-0.0863	-0.0823	0.0560	0.0464
r_4	$2p_Z$	-0.0205	0.0142	0.0130	-0.0071
r_5	$2p_Z$	0.0721	0.0705	-0.0477	-0.0408
s_1	$2p_Z$	0.0721	-0.0705	-0.0485	0.0402
s_2	$2p_Z$	-0.0205	-0.0142	0.0143	0.0082
s_3	$2p_Z$	-0.0863	0.0823	0.0572	-0.0465
s_4	$2p_Z$	-0.0205	-0.0142	0.0130	0.0059
s_5	$2p_Z$	0.0725	-0.0708	-0.0502	0.0424

The interaction between two magnetic sites 1 and 2, is generally expressed by Heisenberg spin Hamiltonian

$$\hat{H} = -2J\hat{S}_1 \bullet \hat{S}_2 \qquad (1)$$

Where $\hat{S}_1$ and $\hat{S}_2$ are the respective spin angular momentum operators and J is the exchange coupling constant. The positive value of J indicates the ferromagnetic interaction while the negative value indicates the antiferromagnetic interaction between two magnetic sites. For a diradical containing one unpaired electron on each site, J can be represented as:

$$E_{(S=1)} - E_{(S=0)} = -2J. \qquad (2)$$

Many researchers[21-28] have developed different formalisms to evaluate *J* using unrestricted spin polarized broken symmetry (BS) solution, depending on the extent of magnetic interaction between two magnetic sites. The equation for evaluating *J* proposed by Ginsberg[23] Noodleman[24] and Davidson[25] is applicable when interaction between two magnetic orbitals is small. On the other hand the expression proposed by Bencini[26,27] and co workers and Ruitz et al.[28] is applicable for large interaction. Nevertheless, the well known expression given by Yamaguchi[29] is applicable for both strong and weak overlap limits. Following the well established[30,31] and widely applied method,[30-35] we use the Yamaguchi [29] formula for evaluation of *J* in this work, which is given by:

$$J = \frac{(E_{BS} - E_{HS})}{\langle S^2 \rangle_{HS} - \langle S^2 \rangle_{BS}} \tag{3}$$

Where E_{BS}, E_{HS} and $\langle S^2 \rangle_{BS}$, $\langle S^2 \rangle_{HS}$ are the energy and average spin square values for corresponding BS and high spin states.

3.3 Results and discussion

3.3.1 Transport properties of the molecular wires 1 and 2

Zero bias transmission spectra of the molecular wires are given in Figure 3.6. The horizontal axis corresponds to the electron energy *E* incident from the electrode. The Fermi energy of bulk gold is −5.53 eV.[36] but a Fermi energy of −5.0 eV is used from DFT calculations.[37] For our calculation the Fermi energy is taken to be −5.0 eV.

We can see from Figure 3.6 that the molecular wire 1 has higher transmission near the Fermi level compared to the molecular wire 2, which implies that the smaller wire is more efficient for electrical transport.[2]

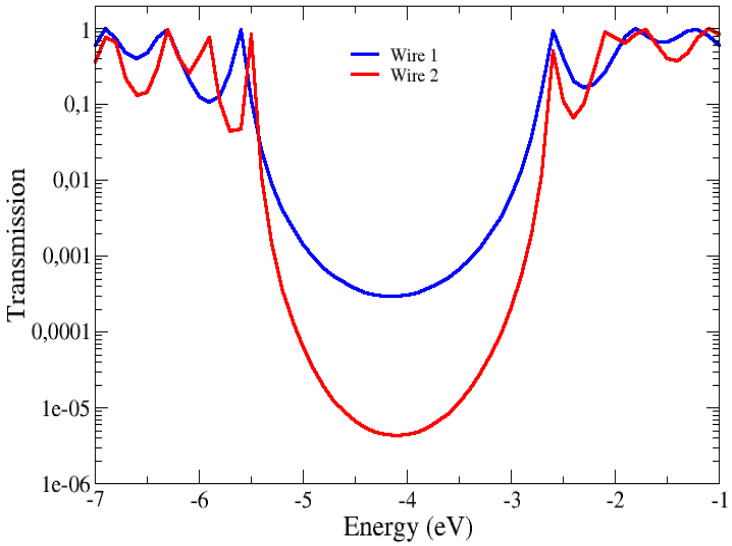

Figure 3.6 Transmission spectra of the molecular wire 1 and molecular wire 2 at zero bias.

Now from the structures of the two molecular wires one may expect that the conductivity of a system increases with increasing the number of π electrons. But organic molecules are not usually very rigid. The flexing and bending of bonds change the overlap between different orbitals. If all the benzene rings in the molecule are in the same plane, the *p* orbitals have maximum overlap that leads to lowest resistance. On the other hand the complete misalignment between the rings leads to highest resistance. The decrease in transmission with the increase in the length of the wire can also be explained by Pauling's bond order[38] which is proportional to the transmission. According to this concept with increasing phenyl ring in a molecular wire Pauling's bond order decreases exponentially and hence the transmission is also decreased.

3.3.2 Molecular orbitals of wire 1 and 2

Molecular orbitals contain all the quantum mechanical information about electronic structures of a molecule. To understand the transport property through a molecule it is necessary to study the molecular orbitals because they offer spatial conduction channels for electron transport.[39] Localization of orbitals can significantly change the transport properties. External electric field is an appropriate stimulus to tune the MOs of a molecule. It has been shown that the MOs of a molecule with and without electrode atoms at their end have similar characteristics under external electric field.[40] Following this analogy and following one of our recent works[41] we apply electric field (parallel to the molecule**)** taking the optimized geometry (without thiol groups and lead atoms at their ends) to study the change of molecular orbital under external electric field.

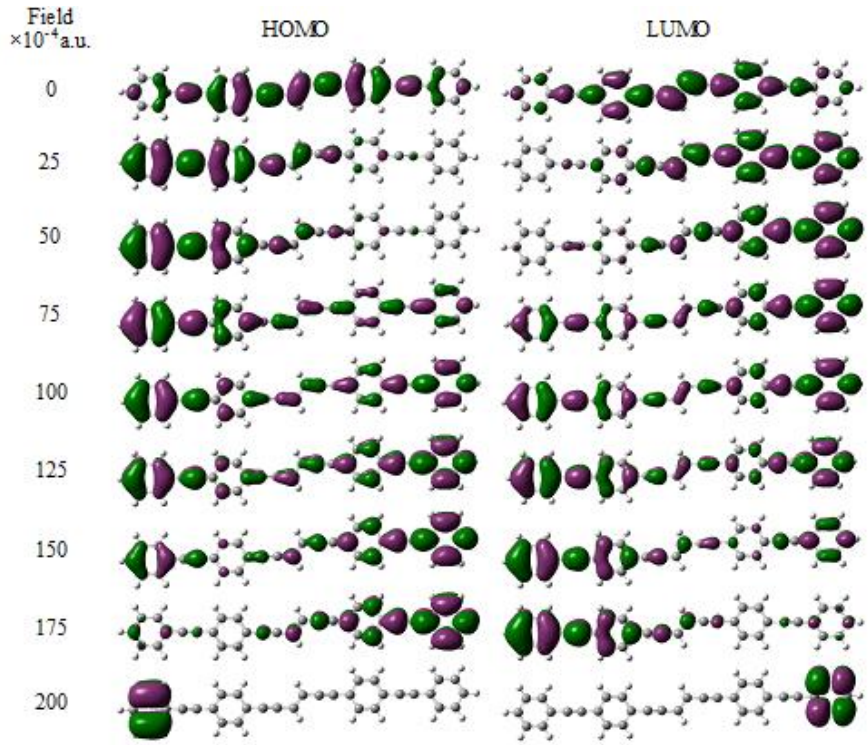

Figure 3.7 Molecular orbitals of the wire 1 under different electric fields.

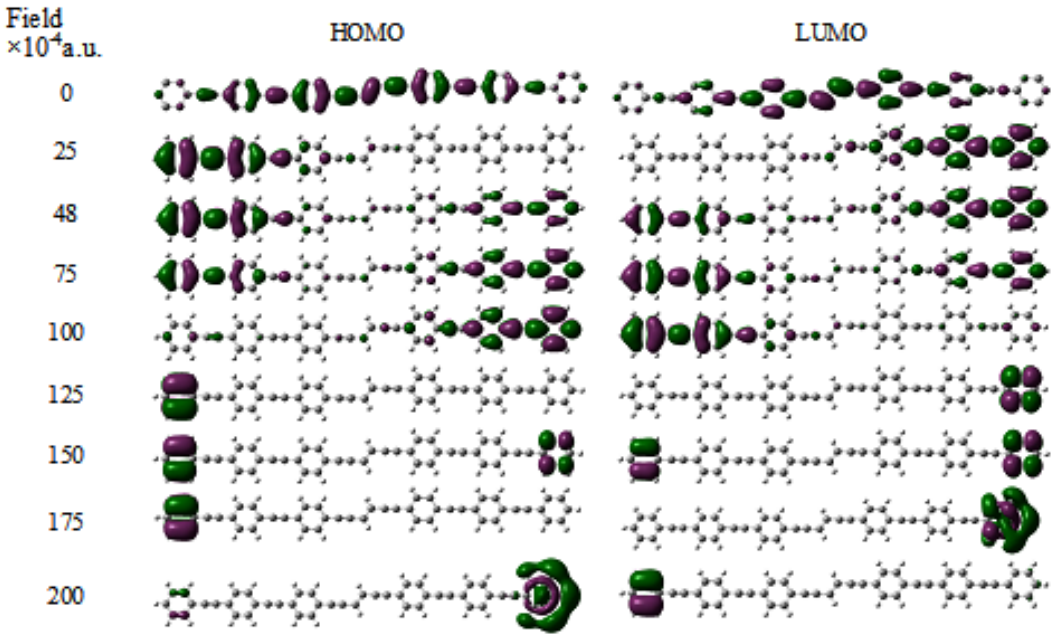

Figure 3.8 Molecular orbitals of the wire 2 under different electric fields.

We can see from Figure 3.7 and Figure 3.8 that at zero external electric field the HOMO and LUMO spreads over the entire molecule. After the application of external electric field MOs are squeezed to few atoms for both the wires. If we closely look at the MOs of wire 1 we can see that the HOMO and the LUMO always collectively spread over all the molecules (except field 0.02 a.u.). However, for wire 2, HOMO and LUMO cannot cover the whole molecule even jointly. Thus with the application of external electric field there is a large separation in the spatial distribution of HOMO-LUMO for molecular wire 2 as compared to wire 1.

3.3.3 Magnetic exchange coupling constant of the diradical substituted molecular wires

We have substituted the molecular wires with two methylene radicals such that the diradical show ferromagnetic and antiferromagnetic interaction according to the spin alternation rule[42] and we change the position of the radicals to vary the distance between the radical centers. The calculated magnetic exchange coupling constant of the diradical are presented in Table 3.2 and Table 3.3. We have also plotted the magnetic exchange coupling constant as a function of the distance between radical centers (Figure 3.9). We can see that with increasing the distance between radical centers magnetic exchange coupling constant value decreases. The distance dependent exchange coupling constant of π–conjugated molecular wires have been studied by Nishizawa et al. and found the similar results.[12]

Table 3.2 The energy (a.u.),$\langle S^2 \rangle$ and magnetic exchange coupling constant (J in cm^{-1}) values of the diradical based molecular wire 1 (B3LYP/6-31G(d,p)).

Diradicals		**Triplet**	**BS**	***J* (cm^{-1})**
1(a)	**Energy (a.u.)**	-1384.81939	-1384.81859	168.83
	$\langle S^2 \rangle$	2.12	1.08	
1(b)	**Energy (a.u.)**	-1384.81940	-1384.81926	30.42
	$\langle S^2 \rangle$	2.08	1.08	
1(c)	**Energy (a.u.)**	-1384.81786	-1384.81784	4.39
	$\langle S^2 \rangle$	2.08	1.08	
1(l)	**Energy (a.u)**	-1384.81813	-1384.81843	-67.38
	$\langle S^2 \rangle$	2.084	1.108	
1(m)	**Energy (a.u.)**	-1384.81680	-1384.81685	-10.21
	$\langle S^2 \rangle$	2.084	1.089	
1(n)	**Energy (a.u.)**	-1384.815334	-1384.81534	-1.58
	$\langle S^2 \rangle$	2.076	1.077	

Table 3.3 The energy (a.u.),$\langle S^2 \rangle$ and magnetic exchange coupling constant (J in cm^{-1}) values of the diradical based molecular wire 2 (B3LYP/6-31G(d,p)).

Diradicals		Triplet	BS	$J(cm^{-1})$
2(a)	Energy (a.u.)	-1999.26030	-1999.25949	169.36
	$\langle S^2 \rangle$	2.123	1.082	
2(b)	Energy (a.u.)	-1999.25952	-1999.25938	30.42
	$\langle S^2 \rangle$	2.10	1.09	
2(c)	Energy (a.u.)	-1999.25940	-1999.25938	4.39
	$\langle S^2 \rangle$	2.09	1.09	
2(d)	Energy (a.u.)	-1999.26018	-1999.26017	2.19
	$\langle S^2 \rangle$	2.08	1.08	
2(e)	Energy (a.u.)	-1999.25866	-1999.25866	0.15
	$\langle S^2 \rangle$	2.078	1.078	
2(l)	Energy (a.u.)	-1999.25951	-1999.26173	-500.10
	$\langle S^2 \rangle$	2.076	1.100	
2(m)	Energy (a.u.)	-1999.25984	-1999.26023	-85.55
	$\langle S^2 \rangle$	2.092	1.107	
2(n)	Energy (a.u.)	-1999.25953	-1999.25959	-14.81
	$\langle S^2 \rangle$	2.089	1.093	
2(o)	Energy (a.u.)	-1999.26034	-1999.26035	-2.57
	$\langle S^2 \rangle$	2.085	1.086	
2(p)	Energy (a.u.)	-1999.26113	-1999.26113	-0.44
	$\langle S^2 \rangle$	2.079	1.079	

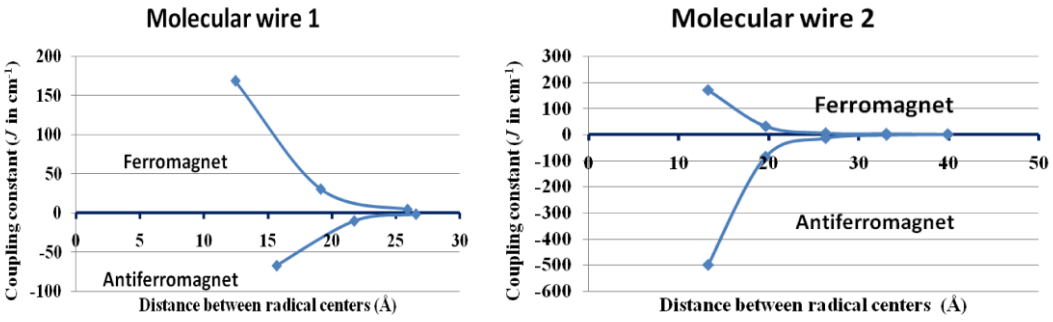

Figure 3.9 Plot of magnetic exchange coupling constants as a function of distance between the radical centers.

3.3.4 Spin density distribution between diradical centers

The spin density of DFT based approach can give us an insight about the spin polarization mechanism in the molecule for magnetic exchange. The spin density of high-spin states of the diradical are represented in Figure 3.10 and Figure 3.11. It is clear that with increasing distance between the radical centers spin polarization decreases; hence the coupling constant also decreases. Therefore, it is obvious that after certain distances between two spin centers spin polarization is no longer effective although the molecule has strong π network. Another important thing is that the magnetic exchange between two spin centers depends only on the environment in between them, not on the outsider substitution.

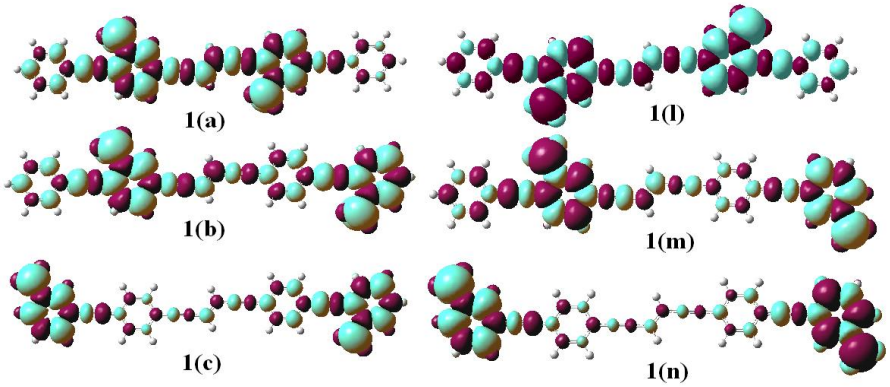

Figure 3.10 Spin density distributions of the ferromagnetically coupled diradicals (high spin state) and antiferromagnetically coupled diradicals (BS state) based on molecular wire 1.

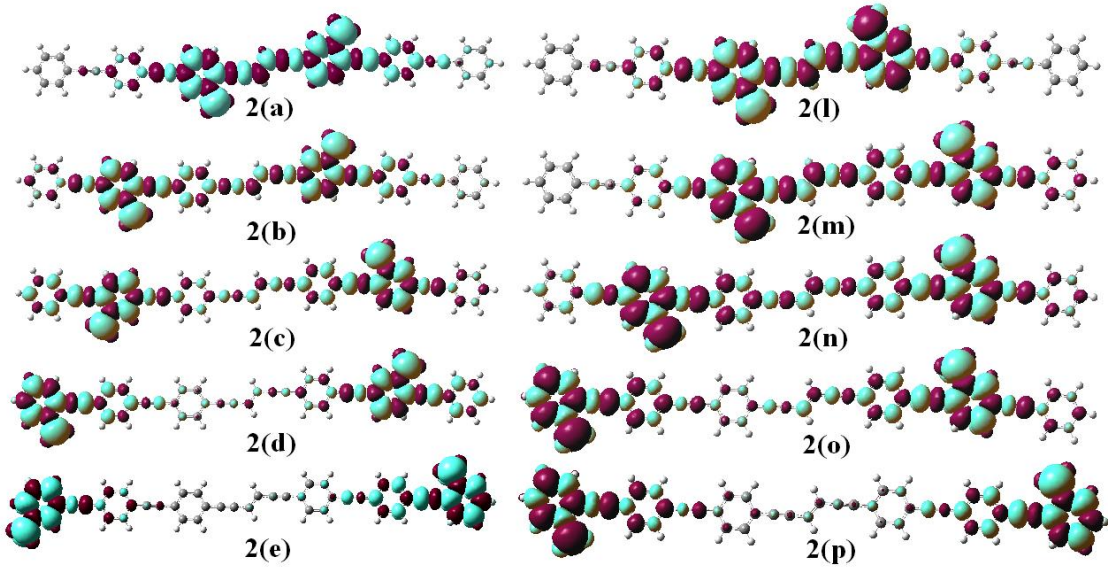

Figure 3.11 Spin density distributions of the ferromagnetically coupled diradicals (high spin state) and antiferromagnetically coupled diradicals (BS state) based on molecular wire 2.

3.3.5 Transport property of the diradical substituted molecular wires

We have studied the transport property of the diradical substituted molecular wires to see the effect of radical substitution on the transport behavior of the molecular wires. The transmission spectra of the diradical substituted wires with varying lengths are presented in Figure 3.12 and Figure 3.13, where we can see that the molecular wires belonging to the same series show almost similar transmission (for ferromagnetically coupled diradicals) however series 1 exhibits higher transmission than series 2. Again comparing the transmission for molecular wire without radical substitution (Figure 3.6), we observe the same result with radical substitution. Hence it can be concluded that the transport property of the molecular wire is independent of radical substitution, whereas, the magnetic exchange coupling constant of the diradical decreases with increasing distance between the radical centers. Stasiw et al. have studied that for donor−bridge−acceptor systems, there is a large variation in magnetic exchange coupling and electronic coupling as a function of bridge conformation.[43] For our designed molecular wires (consist of several aromatic phenyl rings along with radical substitution on the rings), when transmission occurs through the wire, possibly only local transmission of the aromatic rings appear on the Fermi level of the electrode and the radicals are not participated to the transmission of that region, which may be the reason for the same transmission after radical substitution in the ferromagnetic diradicals, but for antiferromagnetic diradicals, there is a small variation in transmission characteristics between radical substituted molecular wires.

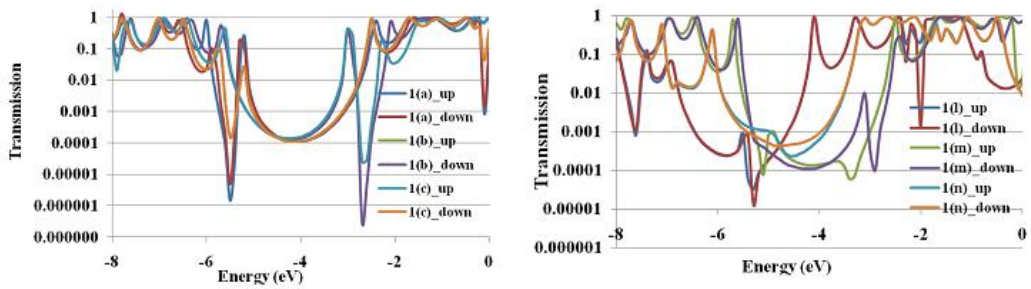

Figure 3.12 The transmission spectra of the diradical substituted molecular wire 1 [1(a)-1(c) high spin state; 1(l)-1(n) BS state].

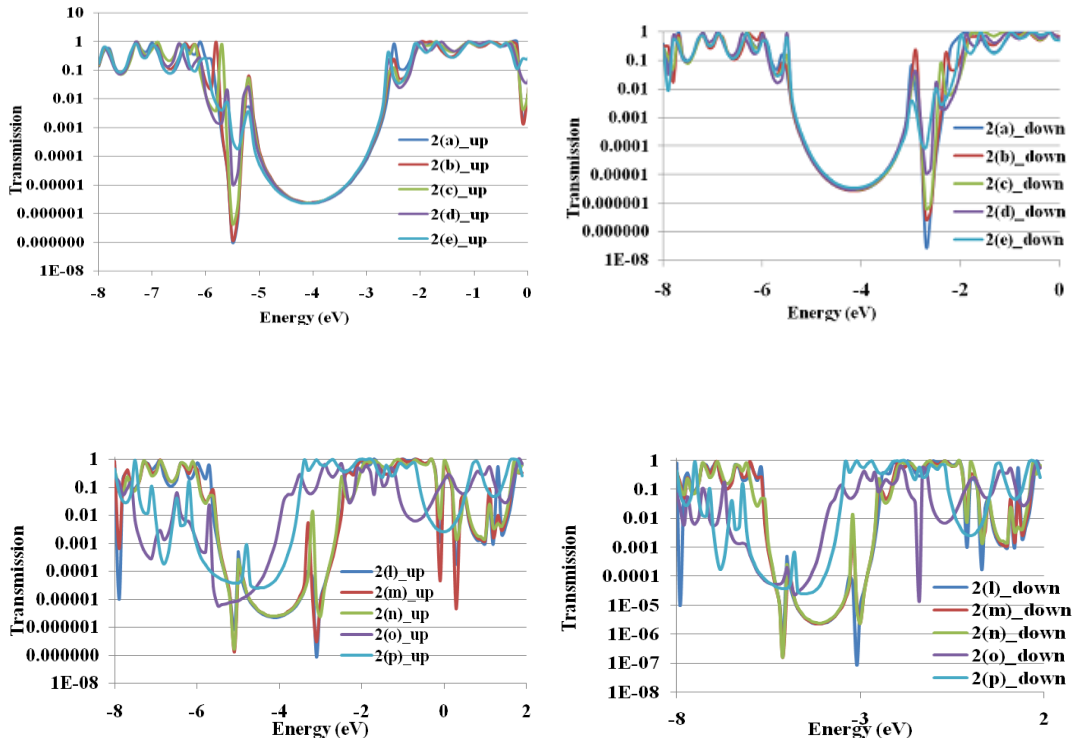

Figure 3.13 The transmission spectra of the diradical substituted molecular wire 2 [2(a)-2(e) high spin state; 2(l)-2(p) BS state].

3.4 Conclusion

To summarize, we studied the effect of the length of molecular wires on the electrical transport properties. We found that the molecular wires (addition polymer) with smaller length show higher transmission, i.e., higher conduction. Another important point is that the magnetic exchange coupling constant of the radical substituted molecular wire depends only on the distance between the spin centers, not on the outsider substitution. The transmission of the molecular wire without radical substitution shows similar observations as that of the wire with radical substitution for ferromagnetically coupled diradicals; however, the transmission characteristics are slightly affected by the antiferromagnetic diradicals.

3.5 References

(1) Tian, W.; Datta, S.; Hong, S.; Reifenberger, R.; Henderson, J. I.; Kubiak, C. P. *J. Chem. Phys.* **1998**, *109*, 2874-2882.
(2) Kober, S.; Gotesman, G.; Naaman, R. *J. Phys. Chem. Lett*. **2013**, *4*, 2041-2045.
(3) Jalili, S.; Rafi-Tabar, H. *Phys. Rev. B* **2005**, *71*, 165410(1-9).
(4) Magoga, M.; Joachim, C. *Phys. Rev. B* **1997**, *56*, 4722-4729.
(5) Durig, U.; Zuger, O.; Michel, B.; Haussling, L.; Ringsdorf, H. *Phys.Rev. B* **1993**, *48*, 1711-1717.
(6) Boulas, C.; Davidovits, J. V.; Rondelez, F.; Vuillaume, D. *Phys. Rev. Lett*. **1996**, *76*, 4797-4800.
(7) Bumm, L. A.; Arnold, J. J.; Cygan, M. T.; Dunbar, T. D.; Burgin, T. P.; Jones, L.; II, Allara, D. L.; Tour, J. M.; Weiss, P. S. *Science* **1996**, *271*, 1705-1707.
(8) Andres, R.P.; Bein, T.; Dorogi, M.; Feng, S.; Henderson, J. I.; Kubiak, C. P.; Mahoney, W.; Osifchin, R.G.; Reifenberger, R.G. *Science* **1996**, *272*, 1323-1325.
(9) Reed, M. A.; Zhou, C.; Muller, C. J.; Burgin, T. P.; Tour, J. M. *Science* **1997**, *278*, 252-254.
(10) Kushmerick, J. G.; Holt, D. B.; Pollack, S. K.; Ratner, M. A.; Yang, J. C.; Schull, T. L.; Naciri, J.; Moore, M. H.; Shashidhar, R. *J. Am. Chem. Soc*. **2002**, *124*, 10654-10655.
(11) Weiss, E. A.; Ahrens, M. J.; Sinks, L. E.; Gusev, A. V.; Ratner, M. A.; Wasielewski, M. R. *J. Am. Chem. Soc.* **2004**, *126*, 5577-5584.
(12) Nishizawa, S.; Hasegawa, J.-Y.; Matsuda, K. *J. Phys. Chem. C* **2013**, *117*, 26280-26286.
(13) Samuel, I. D. W. *Philos. Trans. R. Soc., A,* **2000**, *358*, 193–210.
(14) Lu, H.; Leng, J.; Du, S. *Soft Matter,* **2013**, *9*, 3851–3858.
(15) Lu, H.; Du, S. *Polym. Chem.,* **2014**, *5*, 1155–1162.
(16) Herrmann, C.; Solomon, G. C.; Ratner, M. A. *J. Am. Chem. Soc.* **2010**, *132*, 3682-3684.
(17) Herrmann, C.; Solomon, G. C.; Subotnik, J. E.; Mujica, V.; Ratner, M. A. *J. Chem. Phys.* **2010**, *132*, 024103 (1-17).
(18) Frisch, M. J.; Trucks, G. W.; Schlegel, H. B.; Scuseria, G. E.; Robb, M. A.; Cheeseman, J. R.; Scalmani, G.; Barone, V.; Mennucci, B.; Petersson, G. A.; et.al. Gaussian09; Gaussian, Inc.: Wallingford, CT, **2009**.
(19) Yoshizawa, K. *Acc. Chem. Res.* **2012**, *45*, 1612-1621;
(20) Yoshizawa, K.; Tada, T.; Staykov, A. *J. Am. Chem. Soc*. **2008**, *130*, 9406-9413.
(21) Noodleman, L. *J. Chem. Phys*. **1981**, *74*, 5737.
(22) Noodleman, L.; Baerends, E. J. *J. Am. Chem. Soc*. **1984**, *106*, 2316-2327.
(23) Ginsberg, A. P. *J. Am. Chem. Soc*. **1980**, *102*, 111-117.
(24) Noodleman, L.; Peng, C. Y.; Case, D. A.; Mouesca, J. M. *Coord. Chem. Rev*. **1995**, *144*, 199-244.
(25) Noodleman, L.; Davidson, E. R. *Chem. Phys*. **1986**, *109*, 131-143.

(26) Bencini, A.; Totti, F.; Daul, C. A.; Doclo, K.; Fantucci, P.; Barone, V. *Inorg. Chem*. **1997**, *36*, 5022-5030.
(27) Bencini, A.; Gatteschi, D.; Totti, F.; Sanz, D. N.; McClevrty, J. A.; Ward, M. D. *J. Phys. Chem. A* **1998**, *102*, 10545.
(28) Ruiz, E.; Cano, J.; Alvarez, S.; Alemany, P. *J. Comput. Chem*. **1999**, *20*, 1391-1400.
(29) Yamaguchi, K.; Takahara, Y.; Fueno, T.; Nasu, K. *Jpn. J. Appl. Phys*. **1987**, *26*, L1362.
(30) Ali, Md. E.; Datta, S. N. *J. Phys. Chem. A* **2006**, *110*, 2776-2784.
(31) Ali, Md. E.; Datta, S. N. *J. Phys. Chem. A* **2006,** *110***,** 13232-13237**.**
(*32)* Polo, V.; Alberola, A.; Andres, J.; Anthony, J.; Pilkington, M. Phys. *Chem. Chem. Phys.* **2008**, *10*, 857-864.
(33) Bhattacharya, D.; Misra, A. *J. Phys. Chem. A* **2009,** *113*, 5470-5475**.**
(34) Paul, S.; Misra, A. *THEOCHEM* **2009**, *907*, 35-40.
(35) Paul, S.; Misra, A. *THEOCHEM* **2009**, *895*, 156-160,
(36) Ashcroft, N.W.; Mermin, N.D, Solid *State Physics*, Holt, Rinehart and Winston, New York, **1976**.
(37) F. Pauly, J. K. Viljas, J. C. Cuevas, G. Schön, *Phys. Rev. B,* **2008**, *77*, 155312.
(38) Stuyver, T.; Fias, S.; Proft, De F.; Geerlings, P, *Chem. Phys. Lett.* **2015**, *630*, 51-56.
(39) Kim, W. Y.; Kim, K. S. *Acc. Chem. Res*. **2010**, *43*, 111-120.
(40) Choi, Y. C.; Kim, W. Y.; Park, K. –S.; Tarakeshwar, P.; Kim, K. S.; Kim, T. –S.; Lee, J. Y. *J. Chem. Phys*. **2005**, *122*, 094706 (1-6).
(41) Shil, S.; Misra, A. *RSC Adv.* **2013**, *3*, 14352-14362.
(42) Trindle, C.; Datta, S. N. *Int. J. Quantum Chem.* **1996**, *57*, 781-799.
(43) Stasiw, D. E.; Zhang, J.; Wang, G.; Dangi, R.; Stein, B. W.; Shultz, D.A.; Kirk, M.L.; Wojtas, L.; Sommer, R. D. *J. Am. Chem.Soc*. **2015**, *137*, 9222-9225.